MCB
Journals.ASM.org

Rad51-Dependent Aberrant Chromosome Structures at Telomeres and Ribosomal DNA Activate the Spindle Assembly Checkpoint

Akemi Nakano,[a] Kenta Masuda,[a] Taisuke Hiromoto,[a] Katsunori Takahashi,[a] Yoshitake Matsumoto,[a] Ahmed G. K. Habib,[a] Ahmed G. G. Darwish,[a,b] Masashi Yukawa,[a] Eiko Tsuchiya,[a] Masaru Ueno[a]

Department of Molecular Biotechnology, Graduate School of Advanced Sciences of Matter, Hiroshima University, Higashi-Hiroshima, Japan[a]; Department of Biochemistry, Faculty of Agriculture, Minia University, Minia, Egypt[b]

The spindle assembly checkpoint (SAC) monitors defects in kinetochore-microtubule attachment or lack of tension at kinetochores and arrests cells at prometaphase. In fission yeast, the double mutant between *pot1*Δ and the helicase-dead point mutant of the RecQ helicase Rqh1 gene (*rqh1-hd*) accumulates Rad51-dependent recombination intermediates at telomeres and enters mitosis with those intermediates. Here, we found that SAC-dependent prometaphase arrest occurred more frequently in *pot1*Δ *rqh1-hd* double mutants than in *rqh1-hd* single mutants. SAC-dependent prometaphase arrest also occurred more frequently in *rqh1-hd* single mutants after cells were released from DNA replication block compared to the *rqh1-hd* single mutant in the absence of exogenous insult to the DNA. In both cases, Mad2 foci persisted longer than usual at kinetochores, suggesting a defect in kinetochore-microtubule attachment. In *pot1*Δ *rqh1-hd* double mutants and *rqh1-hd* single mutants released from DNA replication block, SAC-dependent prometaphase arrest was suppressed by the removal of the recombination or replication intermediates. Our results indicate that the accumulation of recombination or replication intermediates induces SAC-dependent prometaphase arrest, possibly by affecting kinetochore-microtubule attachment.

The spindle assembly checkpoint (SAC) monitors defects in kinetochore-spindle interactions (1). Proteins involved in the SAC, such as Bub1 and Mad2, are conserved from yeast to humans (2). Bub1 binds to kinetochores that are not under tension (3). In contrast, Mad2 binds to unattached kinetochores (4). When proper kinetochore-spindle attachment is achieved, the anaphase-promoting complex/cyclosome (APC/C) is activated, which degrades APC substrates such as securin (Cut2 in *Schizosaccharomyces pombe*), allowing anaphase to proceed. The DNA damage checkpoint detects DNA damage and arrests the cell cycle, which provides time for cells to repair DNA before they enter mitosis. In *S. pombe*, the DNA damage checkpoint is activated by the recruitment of Rad3 and other proteins to sites of DNA double-strand breaks (5, 6). Rad3 phosphorylates and activates the downstream effecter kinase Chk1. When the DNA damage checkpoint is activated, Chk1 phosphorylates Cdc25 and Wee1, which maintain Cdc2 in an inactive state, resulting in cell cycle arrest at the G_2/M transition (7–10). A link between DNA damage and the SAC in many organisms, including *Saccharomyces cerevisiae*, *Schizosaccharomyces pombe*, *Drosophila*, and humans (11–18), has been suggested. However, the molecular details of this link are not well understood.

Chromosome ends are protected by several telomere-binding proteins. In *S. pombe*, the double-stranded telomere-binding protein Taz1 and the single-stranded telomere-binding protein Pot1 play important roles in telomere maintenance (19). Deletion of *taz1*$^+$ causes massive telomere elongation (20). Although cell viability is unaffected by *taz1* deletion under standard growth conditions (30 to 32°C), telomere entanglement in *taz1* disruptants makes the cells sensitive to low temperatures (20°C) (21). At 20°C, mitosis is delayed in *taz1* disruptants, and Bub1, but not Mad2, is required for cell survival. This suggests that telomere entanglement disrupts chromosome segregation and that Bub1 helps maintain viability at 20°C (21). Deletion of *pot1*$^+$ causes rapid telomere loss and chromosome circularization (22). Rqh1 suppresses recombination and promotes the resolution of recombination intermediates (23–28). Double mutants between *pot1*Δ and the Rqh1 helicase-dead (*rqh1-hd*) point mutant, in which lysine 547 is mutated to alanine, maintain chromosome ends by homologous recombination (HR) (29). The recombination intermediates exist at chromosome ends even in M phase, which makes cells sensitive to the antimicrotubule drug thiabendazole (TBZ). One study has shown that telomere dysfunction activates the SAC in *Drosophila* (30). However, fly telomeres are maintained by transposons and do not have telomeric sequences. It remains unclear whether telomere dysfunction activates the SAC in organisms that have telomeric sequences.

In this study, we sought to determine whether the accumulation of recombination intermediates at telomeres in the *pot1*Δ *rqh1-hd* double mutant caused defects in M-phase progression. We found that the SAC was activated in the *pot1*Δ *rqh1-hd* double mutant. Bub1 and Mad2 foci persisted longer than usual in the prometaphase-arrested *pot1*Δ *rqh1-hd* double mutant. Moreover, the accumulation of replication intermediates at ribosomal DNA (rDNA) also arrested the cell cycle at prometaphase and activated the SAC. Based on these and other data, we propose that the accumulation of recombination or replication intermediates activates the SAC, possibly by affecting kinetochore-microtubule attachment.

Received 24 December 2013 **Returned for modification** 14 January 2014
Accepted 22 January 2014
Published ahead of print 27 January 2014
Address correspondence to Masaru Ueno, scmueno@hiroshima-u.ac.jp.

doi:10.1128/MCB.01704-13

TABLE 1 *S. pombe* strains used in this study

Strain	Genotype	Source
JY741	*h⁻ leu1-32 ura4-D18 ade6-M216*	M. Yamamoto
JY746	*h⁺ leu1-32 ura4-D18 ade6-M210*	M. Yamamoto
GT000	*h⁺ leu1-32 ura4-D18 ade6-M210 pot1::kanMX6 rqh1-K547A pPC27-pot1⁺-HA*	K. Takahashi et al.
FY18585	*h⁻ leu1 mad2::kanMX6*	NBRP[a]
YK002	*h⁺ leu1-32 ura4-D18 ade6-M210 rqh1-K547A*	K. Takahashi et al.
GT002	*h⁻ leu1-32 ura4-D18 ade6-M210 pot1::kanMX6 rqh1-K547A*	K. Takahashi et al.
TH025	*h⁺ leu1-32 ura4-D18 ade6-M210 pot1::kanMX6 rqh1-K547A (pPC27-Leu-pot1⁺-HA)*	This study
FY10134	*h⁻ leu1 cut2-6×GFP::LEU2*	NBRP
NN439	*h⁻ leu1 mis12-GFP::LEU2*	M. Yanagida
Sp635	*h⁻ leu1 bub1-GFP::kanMX6*	S. Saito
TH002	*h⁻ leu1 bub1-GFP::hphMX6*	This study
FY18581	*h⁻ leu1 bub1::kan MX6*	NBRP
TH026	*h⁺ leu1-32 ura4-D18 ade6-M210 Z:natMX ≪p adh13-mCherry-atb2⁺*	This study
TH003	*h⁺ leu1-32 ura4-D18 ade6-M210 pot1::kanMX6 rqh1-K547A Z:natMX ≪p adh13-mCherry-atb2⁺ (pPC27-pot1⁺-HA)*	This study
pw233	*h⁻ leu1-32 urad4-D18 ade6-M216 kanr≪Padh1-rec8-HA mad2::hphMX6*	Y. Watanabe
TH004	*h⁺ leu1-32 ura4-D18 ade6-M210 rqh1-K547A Z:natMX ≪p adh13-mCherry-atb2⁺*	This study
TH005	*h⁺ leu1-32 ura4-D18 ade6-M210 pot1::kanMX6 rqh1-K547A Z:natMX ≪p adh13-mCherry-atb2⁺*	This study
TH006	*h⁺ leu1-32 ura4-D18 ade6-M210 pot1::kanMX6 rqh1-K547A mad2::hphMX6 Z:natMX ≪p adh13-mCherry-atb2⁺ (pPC27-pot1⁺-HA)*	This study
TH000	*h⁻ bub1::LEU2 ade6-210 leu1-32 ura4-DSE his1-102*	S. W.Wang
TH007	*h⁺ leu1-32 ura4-D18 ade6-M210 pot1::kanMX6 rqh1-K547A mad2::hphMX6 Z:natMX ≪p adh13-mCherry-atb2⁺*	This study
TH008	*h⁺ leu1-32 ura4-D18 ade6-M210 pot1::kanMX6 rqh1-K547A bub1::LEU2 Z:natMX ≪p adh13-mCherry-atb2⁺ (pPC27-pot1⁺-HA)*	This study
TH009	*h⁺ leu1-32 ura4-D18 ade6-M210 pot1::kanMX6 rqh1-K547A bub1::LEU2 Z:natMX ≪p adh13-mCherry-atb2⁺*	This study
TH011	*h⁺ leu1-32 ura4-D18 ade6-M210 pot1::kanMX6 rqh1-K547A mad2::hphMX6 (pPC27-pot1⁺-HA)*	This study
TH012	*h⁺ leu1-32 ura4-D18 ade6-M210 pot1::kanMX6 rqh1-K547A mad2::hphMX6*	This study
TH013	*h⁺ leu1-32 ura4-D18 ade6-M210 pot1::kanMX6 rqh1-K547A bub1::LEU2 (pPC27-pot1⁺-HA)*	This study
TH014	*h⁺ leu1-32 ura4-D18 ade6-M210 pot1::kanMX6 rqh1-K547A bub1::LEU2*	This study
TH015	*h⁻ leu1 ade6-M210 pot1::kanMX6 rqh1-K547A cut2-6×GFP::LEU2 Z:natMX ≪p adh13-mCherry-atb2⁺ (pPC27-pot1⁺-HA)*	This study
TH016	*h⁻ leu1 ade6-M210 pot1::kanMX6 rqh1-K547A cut2-6×GFP::LEU2 Z:natMX ≪p adh13-mCherry-atb2⁺*	This study
TH019	*h⁻ leu1 pot1::kanMX6 rqh1-K547A Z:natMX ≪p adh13-mCherry-atb2⁺ mis12-GFP::LEU2 (pPC27-pot1⁺-HA)*	This study
TH020	*h⁻ leu1 pot1::kanMX6 rqh1-K547A Z:natMX ≪p adh13-mCherry-atb2⁺ mis12-GFP::LEU2*	This study
TH021	*h⁺ leu1-32 ura4-D18 ade6-M210 pot1::kanMX6 rqh1-K547A bub1-GFP::hphMX6 Z:natMX ≪p adh13-mCherry-atb2⁺ (pPC27-pot1⁺-HA)*	This study
TH022	*h⁺ leu1-32 ura4-D18 ade6-M210 pot1::kanMX6 rqh1-K547A bub1-GFP::hphMX6 Z:natMX ≪p adh13-mCherry-atb2⁺*	This study
TH023	*h⁻ leu1 Z:natMX ≪p adh13-mCherry-atb2⁺ bub1-GFP::kanMX6*	This study
TH024	*h⁺ leu1 rqh1-K547A Z:natMX ≪p adh13-mCherry-atb2⁺ bub1-GFP::kanMX6*	This study
MT25	*h⁺ mal3::kanMX6 mad2-GFP-LUE2 bub1-mRFP::kanMx6 his2*	T. Toda
FY18537	*h⁻ leu1-32 ura4-D18 rad51::hphMX6*	NBRP
MBY1747-2	*h⁻ leu1-32 ura4-D18 bub1::ura4*	D. Hirata
AE148	*h⁻ leu1-32 ura4-D18 mad2::ura4*	D. Hirata
AN057	*h⁻ leu1-32 ura4-D18 mad3-GFP:kanMX Z:natMX ≪p adh13-mCherry-atb2⁺ pot::kanMX rqh1K547A*	This study
AN021	*h⁻ leu1-32 ura4-D18 mad3-GFP:kanMX Z:natMX ≪p adh13-mCherry-atb2⁺ pot::kanMX rqh1K547A pPC27 pot1⁺-HA*	This study
AN076	*h⁻ ade6-M210 leu1-32 mad3-GFP:kanMX Z:natMX ≪p adh13-mCherry-atb2⁺ rqh1K547A*	This study
AN092	*h⁻ ade6-M210 leu1-32 ura4-D18 mad2-GFP:LEU2 Z:natMX ≪p adh13-mCherry-atb2⁺ pot::kanMX rqh1K547A*	This study
AN077	*h⁻ ade6-M210 ura4-D18 mad2-GFP:LEU2 Z:natMX ≪p adh13-mCherry-atb2⁺ pot::kanMX rqh1K547A pPC27 pot1⁺-HA*	This study
AN065	*h⁻ ade6-M210 leu1-32 ura4-D18 mad2-GFP:LEU2 Z:natMX ≪p adh13-mCherry-atb2⁺ rqh1K547A*	This study
AN105	*h⁻ ade6-M210 leu1-32 ura4-D18 bub1::ura4 mad2-GFP:LEU2 Z:natMX ≪p adh13-mCherry-atb2⁺ rqh1-K547A*	This study
AN122	*h⁻ ura4-D18 mad2-GFP:LEU2 Z:natMX ≪p adh13-mCherry-atb2⁺ rqh1K547A rad51::hph*	This study
AN106	*h⁺ ade6-D18 leu1-32 cut2-6×GFP::LEU2 Z:natMX ≪p adh13-mCherry-atb2⁺ rqh1-K547A*	This study
AN131	*h⁻ ade6-M210 leu1-32 ura4-D18 Chk1::hph rad11-GFP:kanMX rqh1-K547A*	This study
AN126	*h⁻ ura4-D18 mad2-GFP:LEU2 Z:natMX ≪p adh13-mCherry-atb2⁺ chk1::hph rqh1K547A*	This study
738	*h⁺ chk1d155A:ep ade6-216 leu1-32 ura4-d18*	N. C. Walworth
KTA014	*h⁺ leu1-32 ura4-D18 ade6-M210 pot1::kanMX rqh1-K547A chk1::ura4*	This study
TH010	*h⁺ leu1-32 ura4-D18 ade6-M210 pot1::kanMX rqh1-K547A chk1::ura4 Z:natMX ≪p adh13-mCherry-atb2⁺*	This study
KM005	*H⁺ leu1-32 ura4-D18 ade6-M210 pot1::kanMX rqh1-K547A chk1::ura4 rad11-mRFP::natMX6*	This study
KM003	*h⁻ ura4-D18 pot1::kanMX rqh1-K547A chk1::D155A:ep(HA)*	This study
KM004	*h⁻ ura4-D18 pot1::kanMX rqh1-K547A chk1::D155A:ep(HA) rad11-mRFP::natMX6*	This study
AN216	*h⁻ leu1 pot1::kanMX rqh1-K547A rad51::hph Z:natMX≪p adh13-mCherry-atb2⁺ mis12-GFP::LEU2⁺*	This study
AN200	*h⁺ leu1-32 ura4-D18 ade6-M210 rqh1-K547A Z:natMX ≪p adh13-mcherry-atb2⁺ reb1::kanMX*	This study
D7	*h⁻ leu1-32 ura4-d18 ade6-M210 reb1Δ::kanMX6*	P. Hernandez
AN215	*h? ade6 ura4-D18 leu1 pot1::kanMX rqh1-K547A mis6-2mRFP-hph mad2-GFP-LEU2*	This study
AN207	*h⁻ ade6 ura4-D18 mis6-2mRFP-hph mad2-GFP-LEU2 cut12-cfp-nat rqh1-K547A*	This study

[a] NBRP, National Bio Resource Project.

MATERIALS AND METHODS

Strain construction and growth media. The strains used in this report are listed in Table 1. Strains were constructed by mating or transformation according to previously described procedures (29, 31). To tag the Atb2 protein in *pot1*Δ *rqh1-hd*-related strains with mCherry at the N terminus, pNATZA13-mCherry-*atb2*$^+$ (a gift from Y. Watanabe and T. Sakuno) was linearized with ApaI and used for transformation (32). Cells were grown in YEA medium (0.5% yeast extract, 3% glucose, and 40 μg of adenine/ml) or Edinburgh minimal medium with the required supplements at the indicated temperature (33). For spot assays, cells were grown to 10^7 cells/ml in YEA. Serial dilutions (1:10) were prepared, and 4-μl aliquots were spotted onto plates and incubated at 30°C.

Microscopy. Microscopy images were obtained using an AxioCam digital camera (Zeiss) connected to an Axio Observer.Z1 microscope (Zeiss) with a Plan-Apochromat 63×, numerical aperture (NA) 1.4 objective lens or an αPlan-FLUAR 100×, NA 1.45 objective lens (see Fig. 1A, 1C, 2A, 4B, 5B, and 5C). Pictures were captured and analyzed using AxioVision Rel. 4.8.2 Software (Zeiss). For Fig. 2C, 3A, and 5D, microscopy images were obtained using an iXon3 897 EMCCD camera (Andor) connected to a Yokokawa CSU-W1 spinning-disc scan head (Yokokawa Electric Corp.) and an Olympus IX83 microscope (Olympus) with a UPlanSApo 100× NA 1.4 objective lens (Olympus). Pictures were captured and analyzed using MetaMorph Software (Molecular Devices). A glass-bottom dish (Iwaki) was coated with 5 mg of lectin/ml from *Bandeiraea simplicifolia* BS-I (Sigma). For Fig. 1A, 1C, 2A, 4B, 5B, and 5C, optical section data (3 focal planes with 0.5-μm spacing) were collected, and the best focus plane was used. For Fig. 2C, 3A, and 5D, optical section data (10 focal planes with 0.3-μm spacing, every 30 s) were collected, and the time-lapse sequences were deconvolved using the Huygens image analysis software (Scientific Volume Imaging). The z-stack was then projected using the maximum intensity algorithm of the Huygens image analysis software.

Measurement of telomere length. Telomere length was measured by Southern hybridization according to a previously described procedure (20) with an AlkPhos Direct Labeling and Detection System (GE Healthcare). A telomere associated sequence (TAS1) plus telomere fragment derived from pNSU70 (34) was used as a probe. Genomic DNA was digested with EcoRI, fractioned by 1.5% agarose gel electrophoresis and hybridized to a probe containing the TAS1 plus telomere fragment.

Release from HU arrest. HU (10 mM) was added to an asynchronous culture of mCherry-Atb2-expressing cells in YEA medium at 30°C. After 4 h in HU, the cells were washed and transferred to YEA medium without HU and cultured for a further 2 h at 30°C. The cells were then observed by microscopy.

RESULTS

The SAC is activated in the *pot1*Δ *rqh1-hd* double mutant. The *pot1*Δ *rqh1-hd* double mutant has recombination intermediates at telomeres even in M phase, which may affect the progression of M phase. To examine the phenotype of the *pot1*Δ *rqh1-hd* double mutant in M phase, we analyzed M-phase progression by monitoring the elongation of mitotic spindles in mCherry-Atb2-expressing cells (32). Mitotic spindles elongated normally in >90% of wild-type cells and *rqh1-hd* single mutants (Fig. 1A and B). In contrast, arrest of spindle elongation was detected in ca. 30% of *pot1*Δ *rqh1-hd* double mutants (Fig. 1A and B).

We hypothesized that the arrest of spindle elongation was the result of SAC activation. To test this, we assessed whether the arrest of spindle elongation was Mad2 or Bub1 dependent. Among *pot1*Δ *rqh1-hd mad2*Δ and *pot1*Δ *rqh1-hd bub1*Δ triple mutants, the percentage of spindle elongation-arrested cells was reduced to the wild-type level (Fig. 1B). This suggests that arrest in the *pot1*Δ *rqh1-hd* double mutant is SAC dependent. In fission yeast, securin (Cut2) localizes to the nucleus and mitotic spindles when the SAC is activated, and it is degraded by the APC/C after the SAC is satisfied (35, 36). To confirm that the SAC was activated in prometaphase-arrested *pot1*Δ *rqh1-hd* double mutants, we monitored the Cut2-GFP signal in living cells. In *pot1*Δ *rqh1-hd* double mutants, the Cut2-GFP signal disappeared in cells in which the spindle microtubules elongated normally, whereas the Cut2-GFP signal did not disappear in cells in which spindle microtubule elongation was arrested (Fig. 1C). These data further confirm that the SAC is activated in the *pot1*Δ *rqh1-hd* double mutant.

Prolonged Bub1 and Mad2 focus formation in the *pot1*Δ *rqh1-hd* double mutant. To understand the mechanism of SAC activation in the *pot1*Δ *rqh1-hd* double mutant, the localization of Bub1 and Mad2 was examined. An intense Bub1-GFP kinetochore signal was visible for 2 to 3 min during the very early stage of mitosis (prometaphase) in wild-type cells (37). Similarly, Bub1 foci were visible for 2 to 3 min during prometaphase in the *rqh1-hd* single mutant. In contrast, 79% of the prometaphase-arrested *pot1*Δ *rqh1-hd* double mutants exhibited Bub1 foci for more than 8 min (Fig. 2A and B). Likewise, 72% of the prometaphase-arrested *pot1*Δ *rqh1-hd* double mutants exhibited Mad2 foci for more than 8 min. The Mad2 foci colocalized with Mis6, a kinetochore protein (38), indicating that the Mad2 detected in *pot1*Δ *rqh1-hd* cells localized to kinetochores (Fig. 2C). These data suggest that the *pot1*Δ *rqh1-hd* double mutant has a defect in kinetochore-microtubule attachment.

Kinetochore movement between the two spindle pole bodies (SPBs) in the *pot1*Δ *rqh1-hd* double mutant is prolonged, sug-

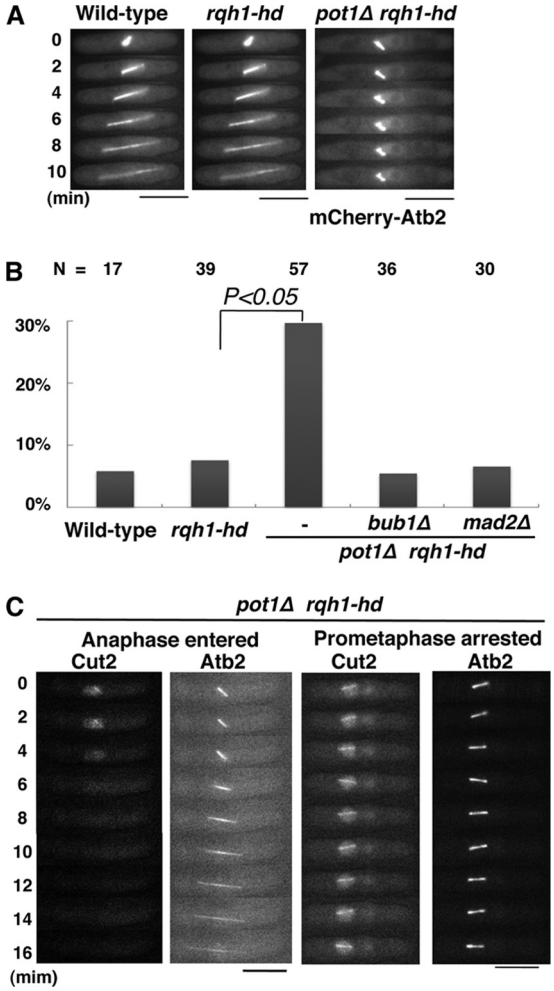

FIG 1 The *pot1*Δ *rqh1-hd* double mutant arrests at prometaphase in a Mad2- and Bub1-dependent manner. (A) Representative time-lapse fluorescence images of the spindle microtubule (mCherry-Atb2) in mCherry-Atb2-expressing wild-type, *rqh1-hd*, and *pot1*Δ *rqh1-hd* cells. Bars, 5 μm. (B) Percentage of prometaphase-arrested cells among mCherry-Atb2-expressing wild-type, *rqh1-hd*, *pot1*Δ *rqh1-hd*, *pot1*Δ *rqh1-hd bub1*Δ, and *pot1*Δ *rqh1-hd mad2*Δ cells. Cells in which spindle elongation arrested for more than 7.5 min were counted as prometaphase-arrested cells. The total cell number examined (N) is shown at the top. (C) Time-lapse fluorescence images of Cut2-GFP and mCherry-Atb2 in *pot1*Δ *rqh1-hd* cells. Left side, *pot1*Δ *rqh1-hd* cells in anaphase; right side, *pot1*Δ *rqh1-hd* cells arrested in prometaphase. Bars, 5 μm.

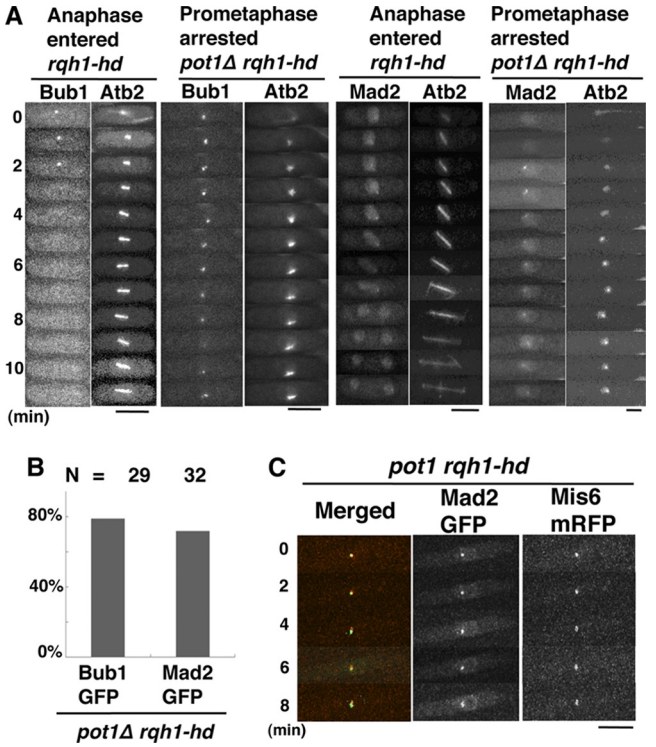

FIG 2 Bub1 and Mad2 foci persist longer than usual in prometaphase-arrested *pot1*Δ *rqh1-hd* cells. (A) Time-lapse fluorescence images of Bub1-GFP or Mad2-GFP and mCherry-Atb2 in *rqh1-hd* cells in anaphase and *pot1*Δ *rqh1-hd* cells arrested in prometaphase. Bars, 5 μm. (B) The percentage of prometaphase-arrested *pot1*Δ *rqh1-hd* cells in which Bub1 or Mad2 foci were present for >8 min. Cells in which spindle elongation was arrested for >7.5 min were counted as prometaphase-arrested cells. The number of prometaphase-arrested *pot1*Δ *rqh1-hd* cells examined (N) is shown at the top. (C) Merged images of fluorescence micrographs showing Mad2-GFP (green) and Mis6-mRFP (red) in prometaphase-arrested *pot1*Δ *rqh1-hd* cells.

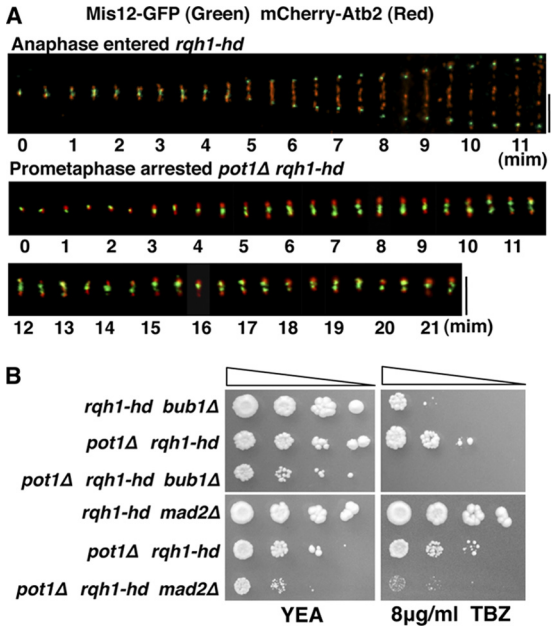

FIG 3 Kinetochores continue to move between the two SPBs in prometaphase-arrested *pot1*Δ *rqh1-hd* cells (A) Merged time-lapse fluorescence images of Mis12-GFP (green) and mCherry-Atb2 (red) in *rqh1-hd* and *pot1*Δ *rqh1-hd* cells. Images were captured every 30 s. Top, *rqh1-hd* cells in anaphase; bottom, *pot1*Δ *rqh1-hd* cells arrested in prometaphase. Bars, 5 μm. (B) Spotting assay using 10-fold serial dilutions of cells. Sensitivity to TBZ was assessed by spotting *pot1*Δ *rqh1-hd*, *pot1*Δ *rqh1-hd bub1*Δ, *rqh1-hd bub1*Δ, *pot1*Δ *rqh1-hd mad2*Δ, and *rqh1-hd mad2*Δ cells onto YEA platesin the absence or presence of the indicated concentrations of TBZ at 30°C.

gesting a defect in kinetochore-microtubule attachment. Our results suggest there is a defect in kinetochore-microtubule attachment in the prometaphase-arrested *pot1*Δ *rqh1-hd* double mutant. If this is true, kinetochores should continue to move between the two SPBs (39). To test this, we examined the localization of the kinetochore in *pot1*Δ *rqh1-hd* double mutants expressing Mis12-GFP (a kinetochore marker [40]) and mCherry-Atb2. In the *rqh1-hd* single mutant, Mis12-GFP signals oscillated between the two ends of the mitotic spindle (SPBs) until all of the kinetochores were attached to microtubules; Mis12-GFP signals then moved rapidly to the SPBs (Fig. 3A). In contrast, Mis12-GFP signals continued to move between the two SPBs in 71% of the prometaphase-arrested *pot1*Δ *rqh1-hd* double mutants ($n = 14$), supporting the conclusion that the double mutant is defective in kinetochore-microtubule attachment (Fig. 3A).

Bub1 and Mad2 are required for the viability of *pot1*Δ *rqh1-hd* cells in the presence or absence of TBZ. The *pot1*Δ *rqh1-hd* double mutant causes prometaphase arrest in Bub1- and Mad2-dependent manners. We next sought to determine whether Bub1 and Mad2 contributed to the viability of the *pot1*Δ *rqh1-hd* double mutant in the presence or absence of TBZ. The *pot1*Δ *rqh1-hd bub1*Δ triple mutant was more sensitive to TBZ than the *pot1*Δ *rqh1-hd* and *rqh1-hd bub1*Δ double mutants (Fig. 3B). Similarly, the *pot1*Δ *rqh1-hd mad2*Δ triple mutant was more sensitive to TBZ than the *pot1*Δ *rqh1-hd* and *rqh1-hd mad2*Δ double mutants (Fig. 3B). Importantly, the growth of the *pot1*Δ *rqh1-hd mad2*Δ and *pot1*Δ *rqh1-hd bub1*Δ triple mutants was less than that of the *pot1*Δ *rqh1-hd* double mutant in the absence of TBZ. These results show that Bub1 and Mad2 are important for the viability of *pot1*Δ *rqh1-hd* cells in the presence or absence of TBZ.

Deletion of *chk1*$^+$ or mutation of the kinase domain in *chk1*$^+$ suppresses TBZ sensitivity and the accumulation of recombination intermediates at telomeres. Our results suggest that recombination intermediates underlie SAC activation in the *pot1*Δ *rqh1-hd* double mutant. To substantiate this hypothesis, we searched for a mutant that suppressed the accumulation of recombination intermediates at telomeres in the *pot1*Δ *rqh1-hd* double mutant. Specifically, because the accumulation of recombination intermediates may underlie the TBZ sensitivity of the *pot1*Δ *rqh1-hd* double mutant (29), we searched for a mutant that suppressed TBZ sensitivity. We found that deletion of *chk1*$^+$ suppressed the TBZ sensitivity of the *pot1*Δ *rqh1-hd* double mutant (Fig. 4A). We then examined the importance of Chk1 kinase activity. We used a *chk1-kd* (kinase dead) point mutant, in which aspartic acid 155 is mutated to alanine, which has no kinase activity *in vitro* (41). The TBZ sensitivity of the *pot1*Δ *rqh1-hd chk1-kd* triple mutant was significantly lower than that of the *pot1*Δ *rqh1-hd* double mutant, demonstrating that the kinase domain of Chk1 is important for the suppression of TBZ sensitivity. Next, we sought to determine whether the deletion of *chk1*$^+$ or mutation of the kinase domain in *chk1*$^+$ suppressed the accumulation of recombination intermediates at telomeres. Foci containing Rad11, a large subunit of replication protein A (RPA), were detected on the

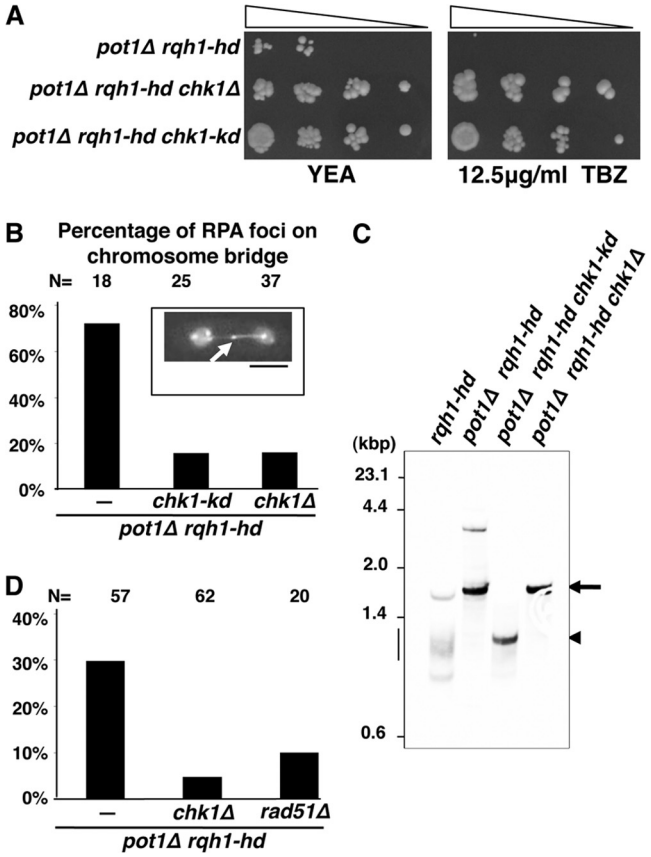

FIG 4 Deletion or mutation of the kinase domain in *chk1*$^+$ suppresses both the accumulation of recombination intermediates at telomeres and the prometaphase arrest of *pot1*Δ *rqh1-hd* double mutants. (A) Deletion or mutation of the kinase domain in *chk1*$^+$ suppressed TBZ sensitivity. A spotting assay using 10-fold serial dilutions of cells was performed. Sensitivity to TBZ was assessed by spotting *pot1*Δ *rqh1-hd*, *pot1*Δ *rqh1-hd chk1*Δ, and *pot1*Δ *rqh1-hd chk1-kd* cells onto YEA plates in the absence or presence of the indicated concentrations of TBZ at 30°C. (B) Percentage of cells in which RPA foci appeared on chromosome bridges (arrow in the box). A representative fluorescence image of a Rad11-mRFP-expressing *pot1*Δ *rqh1-hd* cell, with RPA foci on the chromosome bridge, is shown in the box. Bar, 5 μm. Rad11-mRFP-expressing *pot1*Δ *rqh1-hd*, *pot1*Δ *rqh1-hd chk1*Δ, and *pot1*Δ *rqh1-hd chk1-kd* cells were analyzed. The total cell number examined (N) is shown at the top. (C) Telomere length in *rqh1-hd*, *pot1*Δ *rqh1-hd*, *pot1*Δ *rqh1-hd chk1-kd*, and *pot1*Δ *rqh1-hd chk1*Δ cells was analyzed by Southern hybridization. Genomic DNA was digested with EcoRI, separated by 1.5% agarose gel electrophoresis, and hybridized to a probe containing 300 bp of telomeric DNA and 700 bp of subtelomeric DNA. The bands corresponding to telomeres are indicated by an arrow (for *pot1*Δ *rqh1-hd* and *pot1*Δ *rqh1-hd chk1*Δ), arrowhead (for *pot1*Δ *rqh1-hd chk1-kd*), or bar (for *rqh1-hd*). (D) The percentage of prometaphase-arrested cells in mCherry-Atb2-expressing *pot1*Δ *rqh1-hd*, *pot1*Δ *rqh1-hd chk1*Δ, and *pot1*Δ *rqh1-hd rad51*Δ cells. Cells in which spindle elongation was arrested for >7.5 min were counted as prometaphase-arrested cells. The total cell number examined (N) is shown at the top.

chromosome bridge during M phase in ca. 80% of *pot1*Δ *rqh1-hd* double mutants (Fig. 4B, arrow), suggesting that recombination intermediates accumulate at telomeres even during M phase (29). Deletion or mutation of the kinase domain in *chk1*$^+$ in the *pot1*Δ *rqh1-hd* double mutant significantly reduced the percentage of cells with Rad11 foci on the chromosome bridge during M phase to ca. 20% (Fig. 4B). The reduction in Rad11 foci was not due to a reduction in the amount of single-stranded DNA, at unreplicated regions or single-stranded telomere overhangs, for example, because the percentage of asynchronous *pot1*Δ *rqh1-hd* cells containing Rad11 foci was not affected by deletion of *chk1*$^+$ (data not shown). These results suggest that deletion or mutation of the kinase domain in *chk1*$^+$ suppresses the accumulation of recombination intermediates at telomeres.

Telomeres in *rqh1-hd* cells, which are maintained by telomerase, were detected as broad bands of approximately 1 kbp when chromosomes were digested by EcoRI (Fig. 4C, bar). In contrast, chromosome ends in the *pot1*Δ *rqh1-hd* double mutant are maintained by recombination, and the EcoRI site-containing chromosome ends in the *pot1*Δ *rqh1-hd* double mutant were highly amplified (Fig. 4C, arrow) (29). A similar band pattern was detected for *pot1*Δ *rqh1-hd chk1*Δ cells (Fig. 4C, arrow), suggesting that the chromosome ends are maintained by recombination (Fig. 4C). Although the band size of the *pot1*Δ *rqh1-hd chk1-kd* triple mutant (Fig. 4C, arrowhead) was different from that of the *pot1*Δ *rqh1-hd* and *pot1*Δ *rqh1-hd chk1*Δ cells, a sharp band was detected, implying that the EcoRI site-containing chromosome end fragments were amplified by recombination. Moreover, pulsed-field gel electrophoresis demonstrated that the chromosomes in *pot1*Δ *rqh1-hd chk1-kd* cells were linear (data not shown). Telomeres should be maintained by recombination in the absence of Pot1, because Pot1 is essential for telomerase-dependent telomere maintenance (22, 29). These facts suggest that the chromosome ends in *pot1*Δ *rqh1-hd chk1-kd* cells are still maintained by recombination, and yet no recombination intermediates are accumulated.

Deletion of *chk1*$^+$ or *rad51*$^+$ suppresses the prometaphase arrest of the *pot1*Δ *rqh1-hd* double mutant. We next sought to determine whether the prometaphase arrest of the *pot1*Δ *rqh1-hd* double mutant was suppressed by deletion of *chk1*$^+$. The percentage *pot1*Δ *rqh1-hd* double mutants arrested in prometaphase was significantly reduced by the deletion of *chk1*$^+$ (Fig. 4D), suggesting a link between the accumulation of recombination intermediates and SAC activation.

Because the *pot1*Δ *rqh1-hd rad51*Δ triple mutant has circular chromosomes with no telomeres, the triple mutant has no recombination intermediates at telomeres (29). We sought to determine whether deletion of *rad51*$^+$ suppressed the prometaphase arrest of the *pot1*Δ *rqh1-hd* double mutant. Indeed, deletion of *rad51*$^+$ did suppress prometaphase arrest (Fig. 4D). This further supports a link between recombination intermediates at telomeres and SAC activation in the *pot1*Δ *rqh1-hd* double mutant.

Accumulation of replication intermediates at rDNA loci also activates the SAC. Our results suggest that the accumulation of recombination intermediates at telomeres in the *pot1*Δ *rqh1-hd* double mutant activates the SAC. We next sought to determine whether the accumulation of recombination or replication intermediates at other loci, such as rDNA, also activated the SAC. The *rqh1-hd* single mutant accumulates recombination and replication intermediates at chromosomes, including rDNA loci, and enters mitosis with those intermediates when the cell cycle is released from hydroxyurea (HU)-mediated DNA replication block (24, 27, 42). We analyzed M phase progression in the *rqh1-hd* mutant after release from HU-mediated DNA replication block by monitoring the elongation of the mitotic spindle. The mitotic spindle elongated normally in most *rqh1-hd* single mutants (Fig. 5A). However, arrest of spindle elongation was detected in ca. 40% of the *rqh1-hd* cells released from HU arrest. Moreover, the arrest

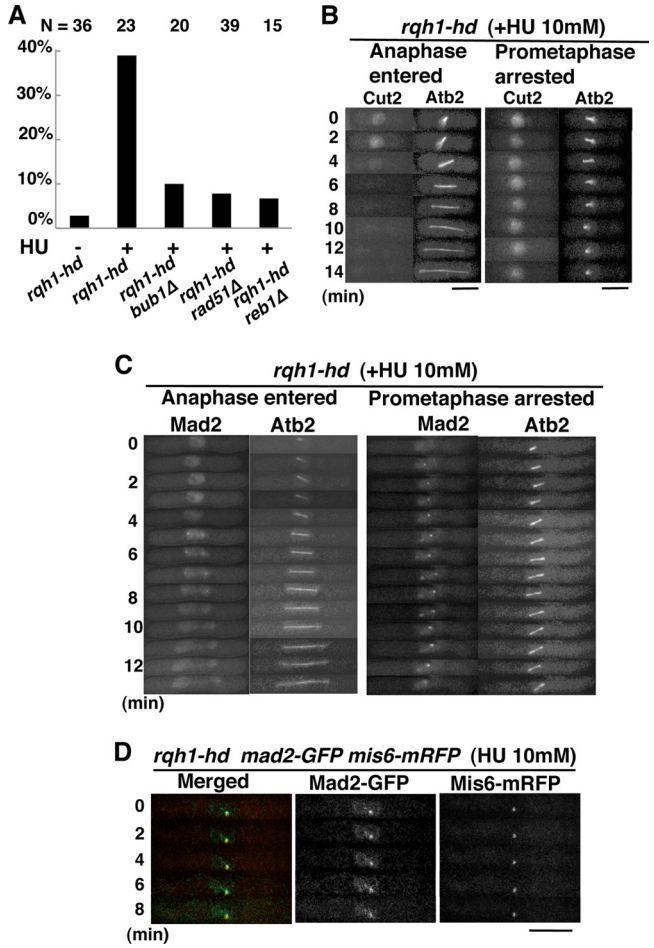

FIG 5 The SAC is activated in *rqh1-hd* cells released from S-phase arrest. (A) Percentage of prometaphase-arrested cells among mCherry-Atb2-expressing *rqh1-hd*, *rqh1-hd bub1*Δ, *rqh1-hd rad51*Δ, and *rqh1-hd reb1*Δ cells released from S-phase arrest. Cells in which spindle elongation was arrested for >7.5 min were counted as prometaphase-arrested cells. The total cell number examined (N) is shown at the top. We added 10 mM HU to asynchronous cultures in YEA medium. After exposure to HU for 4 h, cells were washed and transferred to YEA medium without HU and cultured for a further 2 h. (B) Time-lapse fluorescence images of Cut2-GFP and mCherry-Atb2 in *rqh1-hd* cells released from S-phase arrest. Left, *rqh1-hd* cells in anaphase; right, *rqh1-hd* cells arrested in prometaphase. Bars, 5 μm. (C) Time-lapse fluorescence images of Mad2-GFP and mCherry-Atb2 in *rqh1-hd* cells released from S-phase arrest. Left, *rqh1-hd* cells in anaphase; right, *rqh1-hd* cells arrested in prometaphase. Bar, 5 μm. (D) Merged images of fluorescence micrographs showing Mad2-GFP (green) and Mis6-mRFP (red) in prometaphase-arrested *rqh1-hd* cells released from S-phase arrest.

was Bub1 dependent (Fig. 5A). These results suggest that the accumulation of recombination and replication intermediates at internal chromosomes, including rDNA loci, also activates the SAC.

Given that release from HU-mediated DNA replication block may generate DNA damage in the *rqh1-hd* single mutant in addition to the accumulation of recombination and replication intermediates, DNA damage itself might underlie SAC activation. Deletion of *rad51*$^+$ suppresses aberrant mitosis in *rqh1* mutant cells released from HU arrest, suggesting that Rad51 generates aberrant recombination and replication intermediates in the *rqh1* mutant (43). Thus, deletion of *rad51*$^+$ in *rqh1-hd* would reduce the accumulation of recombination and replication intermediates but not

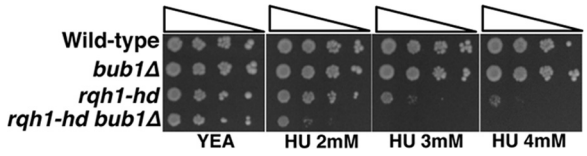

FIG 6 Bub1 contributes to the viability of the *rqh1-hd* mutant in the presence of HU. A spotting assay using 10-fold serial dilutions of cells was performed. Sensitivity to HU was assessed by spotting wild-type, *bub1*Δ, and *rqh1-hd bub1*Δ cells onto YEA plates in the absence or presence of the indicated concentrations of HU at 30°C.

DNA damage itself. To determine that the accumulation of recombination and replication intermediates, but not DNA damage itself, was the reason for SAC activation in *rqh1-hd* cells released from HU arrest, we used the *rqh1-hd rad51*Δ double mutant. Cell cycle progression in the *rqh1-hd rad51*Δ double mutant was monitored after cells were released from HU-mediated arrest. Unlike the *rqh1-hd* single mutant, the *rqh1-hd rad51*Δ double mutant did not arrest in prometaphase, suggesting that recombination and replication intermediates, but not DNA damage itself, are required for SAC activation (Fig. 5A).

The *rqh1* single mutant has defects in rDNA segregation (42). Relieving replication fork arrest at the replication fork barriers by deletion of *reb1*$^+$ suppresses the defect in rDNA segregation, suggesting that the aberrant replication intermediates generated at rDNA loci underlie the rDNA segregation defect in the *rqh1* mutant (42, 44, 45). We sought to determine whether relieving replication fork arrest at the replication fork barriers suppressed prometaphase arrest in *rqh1-hd* cells released from HU-mediated arrest. Interestingly, prometaphase arrest in *rqh1-hd* cells was suppressed by the deletion of *reb1*$^+$ (Fig. 5A). This suggests that the aberrant replication intermediates generated at rDNA loci underlie prometaphase arrest in *rqh1-hd* cells released from HU-mediated arrest.

We also confirmed SAC activation by monitoring Cut2-GFP signals after releasing cells from HU-mediated arrest. In the *rqh1-hd* mutant, the Cut2-GFP signal disappeared in cells in which spindle microtubules elongated normally, whereas the Cut2-GFP signal did not disappear in cells in which spindle microtubule elongation was arrested (Fig. 5B). This further suggests the SAC is activated when replication intermediates accumulate at rDNA loci. Mad2 foci were present for more than 8 min in the prometaphase-arrested *rqh1-hd* mutants (n = 9, 100%), suggesting a defect in kinetochore-microtubule attachment (Fig. 5C). The Mad2 foci detected colocalized with Mis6, a kinetochore protein, demonstrating that Mad2 localized to kinetochores (Fig. 5D).

Bub1 contributes to the viability of the *rqh1-hd* mutant in the presence of HU. Our results suggest that the accumulation of replication intermediates at rDNA results in SAC activation. We next sought to determine whether SAC activation contributed to the viability of *rqh1-hd* mutants exposed to HU, which accumulated recombination and replication intermediates. The *rqh1-hd* single mutant, but not the *bub1* single mutant, was sensitive to HU (46) (Fig. 6). Interestingly, the *rqh1-hd bub1*Δ double mutant was more sensitive to HU than either single mutant, demonstrating that SAC activation by Bub1 contributes to the viability of the *rqh1-hd* mutant in the presence of HU.

DISCUSSION

Recombination intermediates accumulate at telomeres during M phase in the *pot1*Δ *rqh1-hd* double mutant (29). In the present study, we found that the *pot1*Δ *rqh1-hd* double mutant arrested at prometaphase in a manner dependent on Mad2 and Bub1, suggesting that the arrest is SAC-dependent (Fig. 1A and B). Moreover, Cut2 was not degraded in the prometaphase-arrested *pot1*Δ *rqh1-hd* double mutant (Fig. 1C), further supporting SAC activation. The SAC detects defects in kinetochore-microtubule attachment. Bub1 and Mad2 localize to the kinetochore when proper kinetochore-microtubule attachment has not been achieved. Indeed, we found that Bub1 and Mad2 foci persisted for long periods of time in the prometaphase-arrested *pot1*Δ *rqh1-hd* double mutant (Fig. 2). Moreover, Mis12-GFP signals corresponding to kinetochores continued to move between the two SPBs in the prometaphase-arrested *pot1*Δ *rqh1-hd* double mutant (Fig. 3A). These facts suggest that proper kinetochore-microtubule attachment cannot be achieved in the prometaphase-arrested *pot1*Δ *rqh1-hd* double mutant.

We found that deletion of *chk1*$^+$ or mutation of the kinase domain in *chk1*$^+$ suppressed TBZ sensitivity and the accumulation of recombination intermediates at telomeres in the *pot1*Δ *rqh1-hd* double mutant (Fig. 4A and B). These results support our model in which the accumulation of recombination intermediates underlies the TBZ sensitivity of the *pot1*Δ *rqh1-hd* double mutant. It remains unclear how Chk1 contributes to the accumulation of the intermediates. Given that Chk1 is required for cell cycle arrest at the G_2/M transition, deletion of *chk1*$^+$ may reduce the time in which recombination intermediates can accumulate. Another possibility is that Chk1 contributes directly to the recombination-dependent telomere maintenance pathway by controlling the proteins involved in this pathway. Importantly, the prometaphase arrest of the *pot1*Δ *rqh1-hd* double mutant was suppressed by the deletion of *chk1*$^+$ or *rad51*$^+$ (Fig. 4D), suggesting a link between the accumulation of recombination intermediates and SAC activation.

We also found that *rqh1-hd* cells arrested at prometaphase when the cells were released from HU arrest, which causes recombination and replication intermediates to accumulate at chromosome regions, including rDNA loci (Fig. 5A). The arrest was Bub1 dependent (Fig. 5A), and Cut2 was not degraded in prometaphase-arrested *rqh1-hd* cells, suggesting that the SAC is activated under these conditions (Fig. 5B). Neither the *rqh1-hd rad51*Δ double mutant nor the *rqh1-hd reb1*Δ double mutant arrested at prometaphase, suggesting that Rad51-dependent replication intermediates generated at replication fork sites at rDNA loci cause SAC activation (Fig. 5A). The structure of the Rad51-dependent aberrant replication intermediates generated at the rDNA loci remains unclear. Rad51-dependent template exchange occurs during the restart of stalled replication forks in the *rqh1* mutant (47). Therefore, we assume that template exchange between sister chromatids generates the aberrant replication intermediates. Mad2 foci persisted for long periods of time in prometaphase-arrested *rqh1-hd* cells that were released from HU arrest (Fig. 5C). These data suggest that the accumulation of replication intermediates at rDNA in the *rqh1-hd* single mutant also causes a defect in kinetochore-microtubule attachment. The *rqh1-hd bub1*Δ double mutant was more sensitive to HU than either single mutant, suggesting that Bub1 contributes to the viability of the *rqh1-hd* mutant by arresting cells in prometaphase when recombination and/or replication intermediates accumulate (Fig. 6). This emphasizes the importance of SAC activation when aberrant replication intermediates have accumulated. Unlike in the *rqh1-hd bub1*Δ double mutant, the HU sensitivity of the *rqh1 mad2* double mutant is similar to that of each single mutant (42). Thus, Bub1 may be more important than Mad2 for the survival of *rqh1-hd* mutants on HU plates.

Drosophila and vertebrate Chk1 are involved in SAC activation (16, 48, 49). The *S. pombe crb2* mutant arrests in prometaphase in a Chk1-dependent fashion in response to replication stress induced by a topoisomerase I inhibitor (11). We also found that the prometaphase arrest of the *pot1*Δ *rqh1-hd* double mutant was Chk1 dependent. However, the involvement of *S. pombe* Chk1 in the prometaphase arrest of the *pot1*Δ *rqh1-hd* double mutant may be indirect because deletion of *chk1*$^+$ in the *pot1*Δ *rqh1-hd* double mutant suppressed the accumulation of recombination intermediates. Unlike the *pot1*Δ *rqh1-hd* double mutant, prometaphase arrest in *rqh1-hd* cells that were released from HU arrest was not suppressed by the deletion of *chk1*$^+$ or the concomitant deletion of *chk1*$^+$ and *cds1*$^+$ (unpublished data). These results suggest that neither the DNA damage checkpoint nor the replication checkpoint is involved in the SAC-dependent prometaphase arrest of *rqh1-hd* cells released from HU arrest.

Uncapped *Drosophila melanogaster* telomeres activate the SAC (30). In this case, BubR1, a homologue of *S. pombe* Mad3, localizes to uncapped telomeres. However, we detected Mad3 foci only on mitotic spindles in the prometaphase-arrested *pot1*Δ *rqh1-hd* double mutant, suggesting that Mad3 does not localize to telomeres (data not shown). Moreover, we found that the accumulation of replication intermediates at rDNA loci also activated the SAC. Therefore, the mechanism of SAC activation in response to uncapped *D. melanogaster* telomeres may differ from the mechanism of SAC activation in response to the accumulation of recombination or replication intermediates during M phase in *S. pombe*.

In conclusion, our results suggest that recombination intermediates at telomeres or replication intermediates at rDNA activate the SAC, possibly by affecting proper kinetochore-microtubule attachment.

ACKNOWLEDGMENTS

We thank P. Baumann, J. Murray, M. Yanagida, N. Nakazawa, Y. Watanabe, T. Sakuno, T. Toda, D. Hirata, S. Hauf, S. Saitoh, R. Tesin, P. Hernandez, and N. Walworth and the National Bio Resource Project of Japan for providing plasmids and strains. The time-lapse imaging was performed at the Research Center for the Mathematics of Chromatin Live Dynamics of Hiroshima University.

This study was supported by Grants-in-Aid for Scientific Research in Priority Areas from the Ministry of Education, Culture, Sports, Science, and Technology of Japan to M.U.

REFERENCES

1. **Elowe S.** 2011. Bub1 and BubR1: at the interface between chromosome attachment and the spindle checkpoint. Mol. Cell. Biol. **31:**3085–3093. http://dx.doi.org/10.1128/MCB.05326-11.
2. **Kadura S, Sazer S.** 2005. SAC-ing mitotic errors: how the spindle assembly checkpoint (SAC) plays defense against chromosome missegregation. Cell Motil. Cytoskeleton **61:**145–160. http://dx.doi.org/10.1002/cm.20072.
3. **Skoufias DA, Andreassen PR, Lacroix FB, Wilson L, Margolis RL.** 2001. Mammalian mad2 and bub1/bubR1 recognize distinct spindle-

attachment and kinetochore-tension checkpoints. Proc. Natl. Acad. Sci. U. S. A. **98:**4492–4497. http://dx.doi.org/10.1073/pnas.081076898.
4. **Waters JC, Chen RH, Murray AW, Salmon ED.** 1998. Localization of Mad2 to kinetochores depends on microtubule attachment, not tension. J. Cell Biol. **141:**1181–1191. http://dx.doi.org/10.1083/jcb.141.5.1181.
5. **Carr AM.** 2002. DNA structure dependent checkpoints as regulators of DNA repair. DNA Repair (Amst.) **1:**983–994. http://dx.doi.org/10.1016/S1568-7864(02)00165-9.
6. **Humphrey T.** 2000. DNA damage and cell cycle control in *Schizosaccharomyces pombe*. Mutat. Res. **451:**211–226. http://dx.doi.org/10.1016/S0027-5107(00)00051-8.
7. **Finn K, Lowndes NF, Grenon M.** 2012. Eukaryotic DNA damage checkpoint activation in response to double-strand breaks. Cell. Mol. Life Sci. **69:**1447–1473. http://dx.doi.org/10.1007/s00018-011-0875-3.
8. **Langerak P, Russell P.** 2011. Regulatory networks integrating cell cycle control with DNA damage checkpoints and double-strand break repair. Philos. Trans. R. Soc. Lond. B Biol. Sci. **366:**3562–3571. http://dx.doi.org/10.1098/rstb.2011.0070.
9. **Raleigh JM, O'Connell MJ.** 2000. The G_2 DNA damage checkpoint targets both Wee1 and Cdc25. J. Cell Sci. **113**(Pt 10)**:**1727–1736.
10. **Rhind N, Furnari B, Russell P.** 1997. Cdc2 tyrosine phosphorylation is required for the DNA damage checkpoint in fission yeast. Genes Dev. **11:**504–511. http://dx.doi.org/10.1101/gad.11.4.504.
11. **Collura A, Blaisonneau J, Baldacci G, Francesconi S.** 2005. The fission yeast Crb2/Chk1 pathway coordinates the DNA damage and spindle checkpoint in response to replication stress induced by topoisomerase I inhibitor. Mol. Cell. Biol. **25:**7889–7899. http://dx.doi.org/10.1128/MCB.25.17.7889-7899.2005.
12. **Dotiwala F, Harrison JC, Jain S, Sugawara N, Haber JE.** 2010. Mad2 prolongs DNA damage checkpoint arrest caused by a double-strand break via a centromere-dependent mechanism. Curr. Biol. **20:**328–332. http://dx.doi.org/10.1016/j.cub.2009.12.033.
13. **Kim EM, Burke DJ.** 2008. DNA damage activates the SAC in an ATM/ATR-dependent manner, independently of the kinetochore. PLoS Genet. **4:**e1000015. http://dx.doi.org/10.1371/journal.pgen.1000015.
14. **Mikhailov A, Cole RW, Rieder CL.** 2002. DNA damage during mitosis in human cells delays the metaphase/anaphase transition via the spindle-assembly checkpoint. Curr. Biol. **12:**1797–1806. http://dx.doi.org/10.1016/S0960-9822(02)01226-5.
15. **Royou A, Macias H, Sullivan W.** 2005. The *Drosophila* Grp/Chk1 DNA damage checkpoint controls entry into anaphase. Curr. Biol. **15:**334–339. http://dx.doi.org/10.1016/j.cub.2005.02.026.
16. **Su TT.** 2011. Safeguarding genetic information in *Drosophila*. Chromosoma **120:**547–555. http://dx.doi.org/10.1007/s00412-011-0342-9.
17. **Sugimoto I, Murakami H, Tonami Y, Moriyama A, Nakanishi M.** 2004. DNA replication checkpoint control mediated by the spindle checkpoint protein Mad2p in fission yeast. J. Biol. Chem. **279:**47372–47378. http://dx.doi.org/10.1074/jbc.M403231200.
18. **Yang C, Wang H, Xu Y, Brinkman KL, Ishiyama H, Wong ST, Xu B.** 2012. The kinetochore protein Bub1 participates in the DNA damage response. DNA Repair (Amst.) **11:**185–191. http://dx.doi.org/10.1016/j.dnarep.2011.10.018.
19. **Jain D, Cooper JP.** 2010. Telomeric strategies: means to an end. Annu. Rev. Genet. **44:**243–269. http://dx.doi.org/10.1146/annurev-genet-102108-134841.
20. **Cooper JP, Nimmo ER, Allshire RC, Cech TR.** 1997. Regulation of telomere length and function by a Myb-domain protein in fission yeast. Nature **385:**744–747. http://dx.doi.org/10.1038/385744a0.
21. **Miller KM, Cooper JP.** 2003. The telomere protein Taz1 is required to prevent and repair genomic DNA breaks. Mol. Cell **11:**303–313. http://dx.doi.org/10.1016/S1097-2765(03)00041-8.
22. **Baumann P, Cech TR.** 2001. Pot1, the putative telomere end-binding protein in fission yeast and humans. Science **292:**1171–1175. http://dx.doi.org/10.1126/science.1060036.
23. **Caspari T, Murray JM, Carr AM.** 2002. Cdc2-cyclin B kinase activity links Crb2 and Rqh1-topoisomerase III. Genes Dev. **16:**1195–1208. http://dx.doi.org/10.1101/gad.221402.
24. **Doe CL, Dixon J, Osman F, Whitby MC.** 2000. Partial suppression of the fission yeast *rqh1*$^-$ phenotype by expression of a bacterial Holliday junction resolvase. EMBO J. **19:**2751–2762. http://dx.doi.org/10.1093/emboj/19.11.2751.
25. **Murray JM, Lindsay HD, Munday CA, Carr AM.** 1997. Role of *Schizosaccharomyces pombe* RecQ homolog, recombination, and checkpoint genes in UV damage tolerance. Mol. Cell. Biol. **17:**6868–6875.
26. **Onoda F, Seki M, Miyajima A, Enomoto T.** 2001. Involvement of *SGS1* in DNA damage-induced heteroallelic recombination that requires *RAD52* in *Saccharomyces cerevisiae*. Mol. Gen. Genet. **264:**702–708. http://dx.doi.org/10.1007/s004380000358.
27. **Stewart E, Chapman CR, Al-Khodairy F, Carr AM, Enoch T.** 1997. *rqh1*$^+$, a fission yeast gene related to the Bloom's and Werner's syndrome genes, is required for reversible S phase arrest. EMBO J. **16:**2682–2692. http://dx.doi.org/10.1093/emboj/16.10.2682.
28. **Watt PM, Hickson ID, Borts RH, Louis EJ.** 1996. *SGS1*, a homologue of the Bloom's and Werner's syndrome genes, is required for maintenance of genome stability in *Saccharomyces cerevisiae*. Genetics **144:**935–945.
29. **Takahashi K, Imano R, Kibe T, Seimiya H, Muramatsu Y, Kawabata N, Tanaka G, Matsumoto Y, Hiromoto T, Koizumi Y, Nakazawa N, Yanagida M, Yukawa M, Tsuchiya E, Ueno M.** 2011. Fission yeast Pot1 and RecQ helicase are required for efficient chromosome segregation. Mol. Cell. Biol. **31:**495–506. http://dx.doi.org/10.1128/MCB.00613-10.
30. **Musaro M, Ciapponi L, Fasulo B, Gatti M, Cenci G.** 2008. Unprotected *Drosophila melanogaster* telomeres activate the spindle assembly checkpoint. Nat. Genet. **40:**362–366. http://dx.doi.org/10.1038/ng.2007.64.
31. **Nanbu T, Takahashi K, Murray JM, Hirata N, Ukimori S, Kanke M, Masukata H, Yukawa M, Tsuchiya E, Ueno M.** 2013. Fission yeast RecQ helicase Rqh1 is required for the maintenance of circular chromosomes. Mol. Cell. Biol. **33:**1175–1187. http://dx.doi.org/10.1128/MCB.01713-12.
32. **Sakuno T, Tada K, Watanabe Y.** 2009. Kinetochore geometry defined by cohesion within the centromere. Nature **458:**852–858. http://dx.doi.org/10.1038/nature07876.
33. **Moreno S, Klar A, Nurse P.** 1991. Molecular genetic analysis of fission yeast *Schizosaccharomyces pombe*. Methods Enzymol. **194:**795–823. http://dx.doi.org/10.1016/0076-6879(91)94059-L.
34. **Sugawara N.** 1988. DNA sequences at the telomeres of the fission yeast *Schizosaccharomyces pombe*. Ph.D. thesis. Harvard University, Cambridge, MA.
35. **Kumada K, Nakamura T, Nagao K, Funabiki H, Nakagawa T, Yanagida M.** 1998. Cut1 is loaded onto the spindle by binding to Cut2 and promotes anaphase spindle movement upon Cut2 proteolysis. Curr. Biol. **8:**633–641. http://dx.doi.org/10.1016/S0960-9822(98)70250-7.
36. **Nasmyth K, Peters JM, Uhlmann F.** 2000. Splitting the chromosome: cutting the ties that bind sister chromatids. Science **288:**1379–1385. http://dx.doi.org/10.1126/science.288.5470.1379.
37. **Toyoda Y, Furuya K, Goshima G, Nagao K, Takahashi K, Yanagida M.** 2002. Requirement of chromatid cohesion proteins Rad21/Scc1 and Mis4/Scc2 for normal spindle-kinetochore interaction in fission yeast. Curr. Biol. **12:**347–358. http://dx.doi.org/10.1016/S0960-9822(02)00692-9.
38. **Saitoh S, Takahashi K, Yanagida M.** 1997. Mis6, a fission yeast inner centromere protein, acts during G_1/S and forms specialized chromatin required for equal segregation. Cell **90:**131–143. http://dx.doi.org/10.1016/S0092-8674(00)80320-7.
39. **Tang NH, Takada H, Hsu KS, Toda T.** 2013. The internal loop of fission yeast Ndc80 binds Alp7/TACC-Alp14/TOG and ensures proper chromosome attachment. Mol. Biol. Cell **24:**1122–1133. http://dx.doi.org/10.1091/mbc.E12-11-0817.
40. **Goshima G, Saitoh S, Yanagida M.** 1999. Proper metaphase spindle length is determined by centromere proteins Mis12 and Mis6 required for faithful chromosome segregation. Genes Dev. **13:**1664–1677. http://dx.doi.org/10.1101/gad.13.13.1664.
41. **Capasso H, Palermo C, Wan S, Rao H, John UP, O'Connell MJ, Walworth NC.** 2002. Phosphorylation activates Chk1 and is required for checkpoint-mediated cell cycle arrest. J. Cell Sci. **115:**4555–4564. http://dx.doi.org/10.1242/jcs.00133.
42. **Win TZ, Mankouri HW, Hickson ID, Wang SW.** 2005. A role for the fission yeast Rqh1 helicase in chromosome segregation. J. Cell Sci. **118:**5777–5784. http://dx.doi.org/10.1242/jcs.02694.
43. **Miyabe I, Morishita T, Hishida T, Yonei S, Shinagawa H.** 2006. Rhp51-dependent recombination intermediates that do not generate checkpoint signal are accumulated in *Schizosaccharomyces pombe rad60* and *smc5/6* mutants after release from replication arrest. Mol. Cell. Biol. **26:**343–353. http://dx.doi.org/10.1128/MCB.26.1.343-353.2006.
44. **Krings G, Bastia D.** 2004. swi1- and swi3-dependent and independent replication fork arrest at the ribosomal DNA of *Schizosaccharomyces pombe*. Proc. Natl. Acad. Sci. U. S. A. **101:**14085–14090. http://dx.doi.org/10.1073/pnas.0406037101.

45. **Sanchez-Gorostiaga A, Lopez-Estrano C, Krimer DB, Schvartzman JB, Hernandez P.** 2004. Transcription termination factor reb1p causes two replication fork barriers at its cognate sites in fission yeast ribosomal DNA in vivo. Mol. Cell. Biol. **24:**398–406. http://dx.doi.org/10.1128/MCB.24.1.398-406.2004.
46. **Laursen LV, Ampatzidou E, Andersen AH, Murray JM.** 2003. Role for the fission yeast RecQ helicase in DNA repair in G_2. Mol. Cell. Biol. **23:**3692–3705. http://dx.doi.org/10.1128/MCB.23.10.3692-3705.2003.
47. **Lambert S, Mizuno K, Blaisonneau J, Martineau S, Chanet R, Freon K, Murray JM, Carr AM, Baldacci G.** 2010. Homologous recombination restarts blocked replication forks at the expense of genome rearrangements by template exchange. Mol. Cell **39:**346–359. http://dx.doi.org/10.1016/j.molcel.2010.07.015.
48. **Peddibhotla S, Lam MH, Gonzalez-Rimbau M, Rosen JM.** 2009. The DNA-damage effector checkpoint kinase 1 is essential for chromosome segregation and cytokinesis. Proc. Natl. Acad. Sci. U. S. A. **106:**5159–5164. http://dx.doi.org/10.1073/pnas.0806671106.
49. **Zachos G, Gillespie DA.** 2007. Exercising restraints: role of Chk1 in regulating the onset and progression of unperturbed mitosis in vertebrate cells. Cell Cycle **6:**810–813. http://dx.doi.org/10.4161/cc.6.7.4048.